THE VALIDITY OF THE LIQUID WATER CONTENT APPROXIMATION FOR THE DESCRIPTION OF THE LASER BEAM PROPAGATION THROUGH POLYDISPERSE WATER DROPLET AEROSOLS

A.M. Kucherov

N.E. Zhukovskii Central Aerohydrodynamical Institute, Moscow
Received August 6, 1997

The clearing of polydisperse water droplet aerosol upon exposure to a laser beam at high altitudes in the atmosphere with the wind at low pressures and temperatures is considered. It is shown that the linear dependence between the evaporation rate and the radiation intensity is violated for diffusive–convective and subsonic regimes of evaporation. The aerosol clearing problem is solved with the use of the water droplet size distribution. This solution is compared with the liquid water content approximation. Applicability limits of the liquid water content approximation are extended to include the diffusive regime of evaporation.

In Refs. 1–4 the clearing was described with the help of the smooth liquid water content function $w(\mathbf{r}, t)$, where $\mathbf{r} = (x, y, z)$ is the radius–vector of the observation point, whose physical sense is the liquid water content in a unit volume averaged over the macroscale of the beam radius r_0. The microscale is defined by the water droplet radii $a \ll r_0$. The water droplet size distribution is described by the function $f(\mathbf{r}, a, t)$ (see Refs. 4–10). The radiative transfer equation for the function w (see Refs. 4, 5, and 11–14) is derived from the equation for f for linear dependence between the water droplet evaporation rate and the intensity of the incident radiation. The clearing of the water droplet aerosol in the liquid water content approximation considering self–refraction and thermal self–action of the beam due to gas heating was studied in the context of geometrical (see Refs. 15–18) and wave (see Refs. 19–23) optics. Versions of the analytic Glickler solution (see Refs. 1, 4, and 24) are discussed in Refs. 11–14, where the voluminous experimental results are also presented.

The rate of change of water droplet radius da/dt is proportional to the water vapor flow j from its surface and depends on many parameters. The investigations of the evaporation regimes began in Ref. 25; their classification, including the explosive regime of destruction (see Ref. 26) was given in Refs. 11–24 and 27. The fact that the counter pressure is of primary importance for gas dynamic regimes was established later in Refs. 28–30. As functions of the water droplet evaporation rates on the external boundary of the Knudsen layer, the full set of the evaporation and destruction regimes can be written in increasing order the absorbed radiation intensity, namely, diffusive, diffusive–convective, subsonic, sonic, and explosive. As functions of the water velocities inside the water droplet, the following water droplet heating regimes can be identified in increasing order of the heat release: heat conductive, heat conductive–convective, convective, nonisobaric, and isochoric (see Refs. 31 and 32). The correspondence between evaporation and heating regimes was established in Refs. 32 and 33.

Violation of the linear dependence between the evaporation rate j and the radiation intensity I for all regimes except slow–diffusive one raises the question about the validity of the liquid water content approximation. Satisfactory agreement with the experimental data indicates the possible wider range of application than in the rigorous formulation of the problem. Investigations of the applicability limits for the liquid water content approximation on the microscale of the water droplet radius a is the subject of this paper. The methods for derivation of solutions for the function f (Refs. 34–42) based on analytic relations between f and initial distribution (see Refs. 6, 13, and 34), the application of the solution for the water droplet trajectory, and the direct numerical methods are well known. The last are used here.

Let the function of electromagnetic field u be normalized to $\sqrt{I_0}$, where I_0 is the characteristic intensity $I = u^*u$, the coordinate z along the beam axis be normalized to the path length L, and the transverse coordinates x, y be normalized to the initial beam radius r_0. Then the dimensionless equation of the paraxial wave optics (the nonlinear Schrödinger equation) taken the form

$$-2iF\frac{du}{dz} + \vec{\nabla}_\perp^2 u = F\,[-2iFN_T\rho_1 + iN_b\alpha/\alpha_0]\,u, \quad (1)$$

$$u\big|_{z=0} = u_0(x, y) \equiv \exp(-(x^2 + y^2)/2),$$

$$u\big|_{x,y\to\pm\infty} \to 0. \quad (2)$$

0235-6880/97/12 991-07

Here, $F = 2\pi r_0^2/\lambda L$ is the Fresnel number, λ is the radiation wavelength; $N_b = \alpha_0 L$ is the parameter of radiation extinction by the water droplet aerosol, α is the extinction coefficient, $\alpha|_{t=0} = \alpha_0$; $N_T = Q(r_0/L)^2 (n_0 - 1)/n_0$ is the thermal self-action parameter, n_0 is the refractive index of the unperturbed gas, $Q = (\alpha_e I_0 t_0)/\rho_0 h_0$ is the scale of perturbation of the gas density, $\Delta\rho/\rho_0 = Q\rho_1$, ρ_1 is the dimensionless function of the gas density perturbation, ρ_0 and h_0 are the density and the enthalpy of the unperturbed gas, t_0 is the pulse duration or $t_0 = r_0/V_0$, and V_0 is the velocity of the transverse flow. The x axis is directed along the transverse wind component $V(z)$ (independent of x and y by virtue of the condition $r_0 \ll L$; here $V(z) \equiv V_0$ is taken), and the longitudinal wind component does not influence the clearing. The coefficients of the absorption, extinction, effective absorption, and the efficiency of aerosol evaporation α_a, α, α_e a $\alpha_a(1 - \beta)$, and β, respectively, are

$$\alpha_a(\mathbf{r}, t) \text{ a } \pi N \int_0^\infty a^2 K_a(a) f(a)\, da, \tag{3}$$

$$\alpha(\mathbf{r}, t) \text{ a } \pi N \int_0^\infty a^2 K(a) f(a)\, da,\ K(a) \text{ a } b(a) K_a(a), \tag{4}$$

$$\alpha_e(\mathbf{r}, t) \text{ a } \pi N \int_0^\infty [1 - \beta_a(a)] a^2 K_a(a) f(a)\, da \equiv \alpha_a(1 - \beta), \tag{5}$$

$$\beta_a(a, \mathbf{r}, t) \text{ a } \frac{jH_w}{jH_w + j_T},$$

$$\beta(\mathbf{r}, t) \text{ a } \pi N \int_0^\infty \beta_a a^2 K_a(a) f(a)\, da/\alpha_a. \tag{6}$$

Here, $K(a)$, $K_a(a)$, and $b(a)$ are the extinction and absorption efficiency factors of a single water droplet and their ratio (Refs. 12 and 13), N is the particle number density (here, N a N_0 a const), j and j_T are the densities of mass and heat fluxes from the water droplet surface to the air, H_w is the specific heat of water evaporation. The equation for the function f and its initial distribution have the forms

$$\frac{\partial f}{\partial t} + V(z) \frac{\partial f}{\partial x} + \frac{\partial}{\partial a}\left[f \frac{da}{dt}\right] \text{ a } 0, \quad \int_0^\infty f(a)\, da \text{ a } 1, \tag{7}$$

$$f_0(a_0) \text{ a } \frac{n^{n+1}}{\Gamma(n+1)} \frac{a_0^n}{a_m^{n+1}} \exp\left(-n \frac{a_0}{a_m}\right), \tag{8}$$

where $\Gamma(n)$ is the gamma function. The integral of the function f over the radii a is normalized to unity. The initial distribution f_0 is chosen in the Khrgian–Mazin form (Refs. 42), $n = 2$. The modal (most probable) radius a_m is changed from 0.5 to 5 μm. The homogeneity condition of optical field inside the water droplet $8\pi\kappa a/\lambda \ll 1$ (where $\kappa = 0.0662$ is the absorption index of water, $\lambda = 10.6$ μm) is taken to be true. Heating and the evaporation of the water droplet are described by the following system of equation:

$$\frac{da}{dt} \equiv \frac{\partial a}{\partial t} + V(z) \frac{\partial a}{\partial x} = -\frac{j}{\rho_w}, \quad a|_{t\text{a}0;\ x\text{a}-\infty} \text{ a } a_0, \tag{9}$$

$$\rho_w C_{pw} \frac{dT}{dt} \text{ a } \alpha_d I - \frac{3}{a}\{jH_w + j_T\}, \quad T|_{t\text{a}0;\ x\text{a}-\infty} \text{ a } T_\infty, \tag{10}$$

$$j \text{ a } \begin{cases} \dfrac{\langle \rho D \rangle}{a} \ln\left(\dfrac{1 - Y_\infty}{1 - Y_c}\right), & T_d < T_*, \\ M_c p_c \sqrt{\gamma \mu/(RT_c)}, & T_d \geq T_*, \end{cases} \tag{11}$$

$$j_T \text{ a } j \times \begin{cases} \dfrac{(T_c - T_\infty)\langle k \rangle \langle C_p/k \rangle}{\exp(ja\langle C_p/k \rangle) - 1}, & T_d < T_*, \\ C_p(T_c - T_d) + u_c^2/2, & T_d \geq T_*. \end{cases} \tag{12}$$

Here, ρ_w and C_{pw} are the density and the heat capacity of water; α_d a $3K_a(a)/4a$ is the mean volume absorption coefficient of water droplet; T is the mean volume temperature of the water droplet; T_∞, T_d, and T_c are the temperatures of air, water droplet surface, and water vapor on the external boundary of the Knudsen layer; $T = 381$–375 K ($a = 1$–10 μm) is the temperature separating the diffusive–convective and subsonic regimes of evaporation (Ref. 30); Y_c and Y_∞ are the mass concentrations of water vapor in the Knudsen layer and in ambient air; $\langle \rho D \rangle \langle k \rangle \langle C_p/k \rangle$ is the temperature averaged product of the density of a mixture of water vapor with air by the coefficient of diffusion of water vapor into the air, the thermal conductivity of the mixture, and the ratio of the heat capacity to the thermal conductivity; γ and μ are the adiabatic exponent and the molar mass of water vapor; u_c, c, and $M_c = u_c/c$ are the velocities of water vapor and sound and the Mach number, respectively, on the external boundary of the Knudsen layer; R is the universal gas constant. The procedure for calculating j and j_T is described in Refs. 30–33.

The water droplet, as a rule, evaporates more slowly then heats, so $dT/dt \approx 0$ on the scale of evaporation time. In the approximation of the monodisperse aerosol, a a const a a_m and $\beta_a(a) \approx$ const a β_d are taken. From Eqs.(6) and (9), we obtain

$$\frac{da}{dt} \approx \frac{K_a(a)\, \beta_d\, I}{4\rho_w H_w}. \tag{13}$$

Let us multiply Eq. (9) by $4\pi N \rho_w a^3/3$ and integrate it over the radii a (accounting that

$a^4 f(a)\big|_{a\to\infty} \to 0$). We derive the transfer equation for the function of the liquid water content w

$$w = \frac{4}{3}\pi N \rho_w \int_0^\infty a^3 f(a)\, da, \qquad (14)$$

$$\frac{\partial w}{\partial t} + V(z)\frac{\partial w}{\partial x} = -wI\frac{\alpha_d \beta_d}{\rho_w H_w}, \quad w\big|_{t=0;\, x\to-\infty} = w_0(z). \qquad (15)$$

Thus, the liquid water content approximation is exact for the monodisperse aerosol, the constant efficiency of water droplet evaporation, and the linear dependence described by Eq. (13). The dimensionless equation (15) contains the clearing parameter $N_{vw} = t/t_v$ equal to the ratio of the characteristic heating time of the aerosol t_0 to its characteristic evaporation time $t_v = H_w \rho_w/(\alpha_d I_0 \beta_d)$. In the liquid water content approximation the parameters of extinction and thermal self-action in Eq. (1) are $N_{bw} = \alpha_d \beta(a_m) L$, $N_T = \alpha_d I_0 t_0 (1-\beta_d)(r_0/L)^2 (n_0-1)/(n_0 \rho_0 h_0)$. The parameter of evaporation of a single water droplet $N_{va} = K_a(a)\beta_a(a) I_0 t_0/(4\rho_w H_w a_m)$, $N_{va}(a_m) = N_{vw}/3$ enters dimensionless equation (7). In analogy with the liquid water content approximation we introduce the integral parameter of clearing of the polydisperse aerosol

$$N_v = \int_0^\infty N_{va}(a)\, f(a)\, da. \qquad (16)$$

For the polydisperse aerosol all parameters a, j, I, β_a, T_d, and M_c change and are interconnected. The intensity decreases toward the beam edges and along the beam axis, the water droplet radii decrease as time increases, the temperature of the water droplet surface increases upon heating, and the efficiency of droplet evaporation changes with time even for the monodisperse aerosol model. While using one of the above quantities as a parameter, for example the water vapor flow rate, the Mach number M_c, the intensity I, or the water vapor flow j we can identify in the increasing order of the local intensity I the following regimes of evaporation: diffusive, diffusive-convective, subsonic, and sonic.

The assumption that the parameter β_a is independent of the intensity I and the assumption about linear dependence (13) are strictly satisfied only for low intensities I in the lower limit of the diffusive regime of evaporation and for high intensities in the subsonic and sonic regimes. At great altitudes in the atmosphere, low temperatures T_∞, and low air pressures p_∞ in the course of clearing the conditions can be realized when relatively small changes of water droplet radius a or the intensity I by a factor of 1.5–2 may change the parameter β_a by an order of magnitude. The efficiency of the aerosol clearing significantly decreases. Investigations of the clearing of condensation tracks of stratospheric supersonic aircraft that are being developed now (Refs. 43–45), are centered around the problems of atmospheric pollution and impact of aviation on the atmosphere, face the above-named fact.

The boundaries of the region of nonlinear dependence $j(I)$ at $T_\infty = 253$ K and pressures corresponding to altitudes of 0 and 18 km are drawn on the droplet radius – radiation intensity plane in Fig. 1. In a hot jet stream of the airplane the temperature T_∞ is higher than the atmospheric temperature. The lower solid curve is for a 3% deviation of the dependence $j(I)$ from the linear law in the diffusive regime. The position of this boundary is independent of the pressure, i.e., of the altitude above see level. The upper boundaries (the dashed lines) are for the subsonic regime with $j_T = 0$ and counter air pressure p_∞ corresponding to altitudes of 0 and 18 km. The region where assumption (13) (under which equation of heating of the medium (15) in the liquid water content approximation is obtained) is violated, lies between the upper and the lower boundaries. This region (see Fig. 2) is relatively small at $T_\infty = 293$ K (in it, 10^6 W/m^2 $\le I \le 3\cdot10^7$ W/m^2, $a = 5$ μm); it increases several times at $T_\infty = 253$ K ($6\cdot10^4$ W/m^2 $\le I \le 7\cdot10^7$ W/m^2; $a = 5$ μm) and increases only slightly with the further decrease of the temperature T_∞.

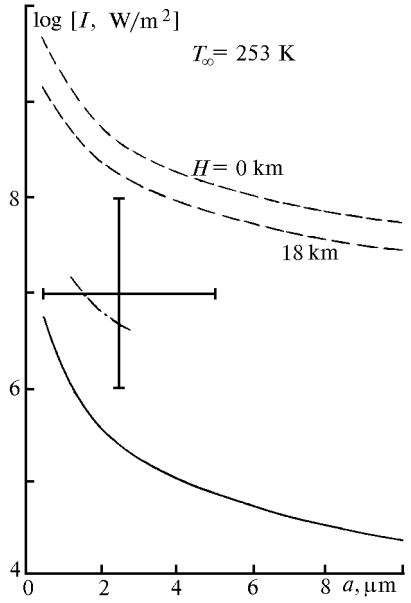

FIG. 1. Boundaries of violation of the linear dependence j(I) between the evaporation rate j and the radiation intensity I in the coordinates radiation intensity I – water droplet radius a. The solid curve is for a 3% deviation in the diffusive regime (altitude range 0–18 km*), the dashed curve is for the subsonic regime ($j_T = 0$ and $\beta_a = 1$ at altitudes of* 0 *and* 18 km*), the dot-dash curve is for the lower boundary of the validity of the liquid water content approximation, and the cross indicates the ranges of variations of the examined parameters. The air temperature was $T_\infty = 253$ K.*

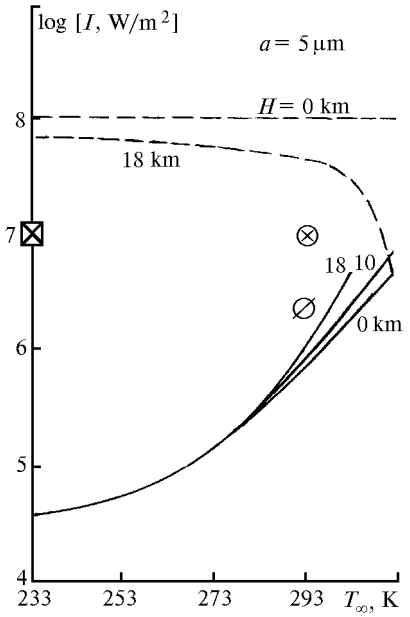

FIG. 2. Boundaries of violation of the linear dependence j(I) in the coordinates radiation intensity I – air temperature T_∞. The water droplet radius was a a 5 μm. *The solid curves are for a* 3% *deviation in the diffusion regime (at altitudes of* 0, 10, *and* 18 km*) and the dashed curves are for the subsonic regime (at altitudes of* 0 *and* 18 km*). The symbols* ⊠, ⊗, *and* ∅ *indicate the ranges of variations of the examined parameters and individual calculations, respectively.*

The above-indicated range of variation of the parameters corresponds to the conditions of forming the clearing channel in the condensation jet stream. The diffusive-convective and subsonic regimes of evaporation are realized for the above-indicated ranges of variations of the intensity (Ref. 30).

Numerous experimental data show that the liquid water content approximation describes satisfactorily the clearing process in the region wider than the region of linear dependence $j(I)$. The algorithm was developed, the computer code was created, and the solutions were obtained for more rigorous physical-mathematical model (Eqs. (1)–(12)) that considered the droplet size distribution and nonlinear relations of all parameters a, j, I, β_a, T_d, and M_c for the purposes of rigorous determination of the applicability limits of the liquid water content approximation and establishing limitations and estimating the errors of calculation of individual physical parameters for this effective model of clearing description. These solutions are then compared with the solution in the liquid water constant approximation (Eqs. (1) and (15)). Details of solution for individual parameters, including spatiotemporal distributions and dependences on the spectrum of particle radii a, are given in Ref. 46. The 4-dimensional evolution problem is solved in the space x, z, a, and t on the grid 64×25×40 with relative steps Δx a 0.1, Δz a 0.04, Δa a 0.1, and Δt a 0.001–0.01. The main difficulty of calculations is joining of the variables j and j_T when going from the diffusive-convective regime to the subsonic one, which occurs at the surface temperature close to that of water boiling.

The solutions are constructed in the liquid water content approximation considering the function of the water droplet size distribution with model radii a_m a 0.5–5 μm (at I_0 a 10^7 W/m^2) for the ranges of variations of the intensity I_0 a 10^6–10^8 W/m^2 (a_m a 2.5 μm) at the pressure p_∞ a $0.0756 \cdot 10^5$ Pa (at an altitude of 18 km) and the temperature T_∞ a 233 K (the intervals of particle radii and the range of variation of the intensity are marked by the cross in Fig. 1 and by the cross in the square in Fig. 2). The individual calculations, performed at an altitude of 0 km and T_∞ a 293 K, are marked by the symbols ⊗ and ∅ in Fig. 2.

The initial liquid water content was identical for two approaches w_0 a $3.14 \cdot 10^{-4}$ kg/m^3 and constant in the above-named runs of calculations (the particle number density N_0 a 10^8–10^{13} m^{-3} with a_m a 5–0.5 μm). The extinction coefficient and the clearing and thermal self-action parameters N_{bw}, N_{vw}, and N_T, as well as the quantity β_d for the liquid water content approximation were calculated at a a a_m. The parameter of thermal self-action was small. So we took ρ_1 a 0 (thought the code allows one to consider the thermal self-refraction), the air flow velocity V_0 a 1.5 m/s, the beam radius r_0 a 0.05 m, and the path length L a 20 m. The diffraction beam broadening on such paths is negligible.

The common regularities of variations of the quantities f and β should be pointed out. The maximum of the function f increases and shifts toward smaller radii a as the time increases and when the observation points moves from the beam edge to the beam axis and from the end point of the propagation path to its initial point, i.e., for increasing local intensity in all cases. The parameter β sharply decreases toward beam edges down to β_{min} and decreases smoother as the time increases and as the observation point moves along the beam axis.

The distributions of the quantities a, f, β, β_a, α, α_a, and α_e, the similarity parameters N_b and N_v (as well as N_T in order to follow the tendency of changing), and the output parameters, namely, the radiation intensity I and the optical thickness of the medium τ a $\int_0^L \alpha \, dz$ have been analyzed. The integral (over the water droplet radii) parameters β, N_b, and N_v decrease with the increase of time and along the path. The parameter N_T increases with the increase of z. The decrease of the water droplet radii is significant for the spectrum of particle radii $a_0 > 2$ μm and insignificant for small water droplets with $a_0 < 1$ μm.

The error of the liquid water content approximation for the examined ranges of variation of the intensity and modal radii is shown in Figs. 3 and 4. The beam intensity I and the optical thickness τ as

functions of the most probable value of the water droplet radius a_m in the range 0.5–5 μm for the initial beam intensity I_0 a 10^7 W/m^2 at the moment of establishing of the clearing process when t/t_0 a 1–2 (t_{phys} a 0.033–0.0667 s) are shown in Fig. 3*a*.

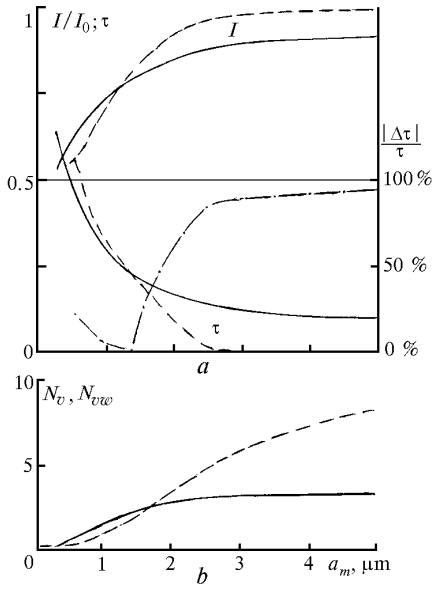

FIG. 3. Comparison of the intensities I/I_0 and optical thickness τ observed at the end point of the path at z a L a 20 m in the polydisperse water droplet aerosol with the initial liquid water content w_0 a $3\cdot10^{-4}$ kg/m^3 calculated considering the water droplet size distribution (the solid curves) and in the liquid water content approximation as functions of the modal radius a_m. The dot–dash curve shows the relative error $\Delta\tau/\tau$ a $(\tau - \tau_w)/\tau$ in calculating the optical thickness τ_w in the liquid water content approximation. The air temperature was I_∞ a 233 K, the characteristic radiation intensity was I_0 a 10^7 W/m^2 (a). Variations of the clearing parameters N_v and N_{vw} as functions of a_m (b).

The dashed line is for the liquid water content approximation, the dot-dash line $\Delta\tau/\tau$ a $(\tau - \tau_w)/\tau$ is for the relative error of calculation of the optical thickness in the liquid water content approximation. The values of the extinction parameters are close: N_b a 0.741–0.654 and N_{bw} a 0.728–0.802 for a_m a 0.5–5 μm. The values of the evaporation parameters N_v and N_{vw} (the dashed lines) are shown in Fig. 3*b*. For $a_m > 2$ μm the parameter N_{vw} is overestimated in the liquid water constant approximation. The aerosol clearing occurs practically till the zero optical thickness τ, while the more exact solution saturates at the fixed nonzero level $\tau \cong 0.1$. This is explained by the significant decrease of the water droplet evaporation efficiency with the decrease of the droplet radii. The clearing process slows down. The relative error $|\Delta\tau|/\tau$ of the calculation of the optical thickness in the liquid water content approximation for $a_m < 1.5$ μm is close to zero and for $a_m > 2.5$ μm it increases up to 85–95% (partly this is caused by the incorrect choice of β_d equal to $\beta_a(a_m)$ for these radii of water droplets).

In the range of the intensity variations I_0 a 10^6–10^8 W/m^2 (a_m a 2.5 μm, Fig. 4*a*), the error of the liquid water content approximation $|\Delta\tau|/\tau$ reaches 100% for $I_0 > 2\cdot10^7$ W/m^2. For $I_0 < 5\cdot10^6$ W/m^2, $|\Delta\tau|/\tau$ decreases down to zero. The liquid water content approximation agrees satisfactorily with the more exact solution considering the water droplet size distribution for $a_m < 1.5$ μm (I_0 a 10^7 W/m^2) and $I_0 < 5\cdot10^6$ W/m^2 (a_m a 2.5 μm).

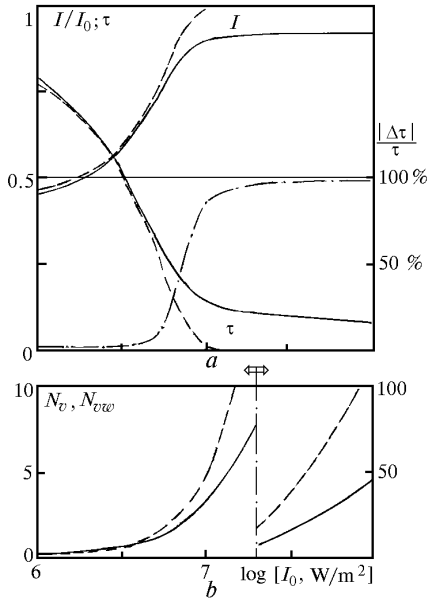

FIG. 4. Dependences of I/I_0, τ, and $\Delta\tau/\tau$ (see Fig. 3a) on the characteristic intensity I_0. The modal radius of the water droplets was a_m a 2.5 μm (a). The clearing parameters N_v and N_{vw} as functions of I_0 (b).

Our investigations extend the applicability limits of the liquid water content approximation from the lower limit of the diffusive regime of evaporation (p_w a β_{min}, the solid line in Fig. 1) to a new boundary ($|\Delta\tau|/\tau \ll 1$, the dot-dash line in Fig. 1). On this boundary, the evaporation parameter is significant: N_v a 2.2 (a_m a 1.5 μm, I_0 a 10^7 W/m^2) and 1.09 (I_0 a $5\cdot10^6$ W/m^2, a_m a 2.5 μm). The quantitative agreement of the evaporation parameters N_v and N_{vw} in the range of small errors of the liquid water content approximation and significant discrepancy in the range of large errors $|\Delta\tau|/\tau$ indicate that for the polydisperse aerosol the parameter N_v can be used as an analog to the parameter N_{vw}. We note that the function $w(x, z, t)$ alone in the liquid water content approximation cannot describe a wide variety of the spatiotemporal distributions of the extinction, absorption, and thermal self-action that enter the equation. The liquid water content approximation

overestimates the thickness and depth of the clearing channel. Application of the liquid water content approximation in cases in which the knowledge of clearing microphysics detail is not critical should be accompanied by the test comparison with the more exact solution considering the water droplet size distribution and the nonlinear dependence between the parameters. Significant discrepancies between two solutions for the diffusive-convective and subsonic regimes of evaporation under examined conditions point to the fact that the applicability of the liquid water content approximation should be checked in other cases as well, including diffraction beam broadening, thermal self-action, variations of initial optical aerosol thickness, and so on.

ACKNOWLEDGMENT

This work was supported in part by the Russian Foundation for Basic Research and MNTC (Project No. 200).

REFERENCES

1. G.L. Lamb and R.B. Kinney, J. Appl. Physics **40**, No. 1, 416–417 (1969).
2. G.W. Sutton, AIAA J. **8**, No. 10, 1907–1910 (1970).
3. A.P. Sukhorukov, R.V. Khokhlov, and E.N. Shumilov, Pis'ma Zh. Eksp. Teor. Fiz. **14**, No. 4, 145–150 (1971).
4. S.I. Glickler, Appl. Optics **10**, No. 3, 644–650 (1971).
5. D.E. Svetogorov, Kvant. Elektron., No. 1(13), 63–69 (1973).
6. A.P. Sukhorukov and E.N. Shumilov, Zh. Tekh. Fiz. **43**, No. 5, 1029–1041 (1973).
7. V.I. Bukatyi, V.E. Zuev, A.V. Kuzikovskii, and S.S. Khmelevtsov, Dokl. Akad. Nauk SSSR **217**, No. 1, 52–55 (1974).
8. V.I. Bukatyi, V.E. Zuev, A.V. Kuzikovskii, M.F. Nebol'sin, and S.S. Khmelevtsov, Dokl. Akad. Nauk SSSR **218**, No. 3, 558–561 (1974).
9. A.V. Korotin, D.E. Svetogorov, Yu.S. Sedunov, and L.P. Semenov, Dokl. Akad. Nauk SSSR **220**, No. 4, 829–832 (1975).
10. M.P. Gordin and G.P. Strelkov, Kvant. Elektron. **3**, No. 11, 2427–2432 (1976).
11. V.E. Zuev, Yu.D. Kopytin, and A.V. Kuzikovskii, *Nonlinear Optics Effects in Aerosols* (Nauka, Novosibirsk, 1980), 116 pp.
12. O.A. Volkovitskii, Yu.S. Sedunov, and P.P. Semenov, *Propagation of the Intensity Laser Radiation through Clouds* (Gidrometeoizdat, Leningrad, 1982), 312 pp.
13. V.E. Zuev, A.A. Zemlyanov, Yu.D. Kopytin, and A.V. Kuzikovskii, *High-Power Laser Radiation in the Atmospheric Aerosol* (Nauka, Novosibirsk, 1984), 223 pp.
14. V.E. Zuev, A.A. Zemlyanov, and Yu.D. Kopytin, *Nonlinear Atmospheric Optics* (Gidrometeoizdat, Leningrad, 1989), 256 pp.
15. V.I. Bukatyi, Yu.D. Kopytin, and S.S. Khmelevtsov, Kvant. Elektron., No. 1(13), 70–74 (1973).
16. S.A. Armand, Radiotekhn. Elektron. **21**, No. 6, 1162–1169 (1976).
17. A.F. Nerushev and L.P. Semenov, Kvant. Elektron. **3**, No. 6, 1226–1232 (1976).
18. A.A. Zemlyanov, V.V. Kolosov, and A.V. Kuzikovskii, Kvant. Elektron. **3**, No. 6, 1148–1154 (1976).
19. K.D. Egorov, V.P. Kandidov, and M.S. Prakhov, Kvant. Elektron. **6,** No. 12, 2562–2566 (1979).
20. F.A. Armand and A.P. Popov, Radiotekhn. Elektron. **25**, No. 9, 1793–1800 (1980).
21. M.P. Gordin and G.M. Strelkov, Radiotekhn. Elektron. **27**, No. 8, 1457–1461 (1982).
22. A.N. Kucherov, Atmos. Oceanic Opt. **7**, No. 10, 749–752 (1994).
23. A.N. Kucherov, Kvant. Elektron. **22**, No. 3, 253–257 (1995).
24. W.H. Arnold, Nuclear Science and Engineering **5**, No. 2, 137 (1959).
25. F.A. Williams, Intern. J. Heat and Mass Transfer **8**, No. 4, 575–587 (1965).
26. A.V. Kuzikovskii, Izv. Vyssh. Uchebn. Zaved. Ser. Fizika, No. 5, 89–94 (1970).
27. V.E. Zuev, A.V. Kuzikovskii, V.A. Pogodaev, S.S. Khmelevtsov, and L.K. Chistyakova, Dokl. Akad. Nauk SSSR **205**, No. 5, 1069–1072 (1972).
28. C.J. Knight, AIAA J. **17**, No. 5, 519–523 (1979).
29. A.V. Butkovskii, Inzh.–Fiz. Zh. **58**, No. 2, 318 (1990) (VINITI, No. 6023–B89).
30. A.N. Kucherov, Teplofiz. Vysokikh Temp. **29**, No. 1, 144–152 (1991).
31. A.N. Kucherov, Inzh.–Fiz. Zh. **61**, No. 2, 253–261 (1991).
32. A.N. Kucherov, Inzh.–Fiz. Zh. **64**, No. 1, 29–34 (1993).
33. A.N. Kucherov, Teplofiz. Vysokikh Temp. **30**, No. 4, 761–768 (1992).
34. M.N. Buikov, Izv. Akad. Nauk SSSR, Fiz. Atmos. Okeana, No. 7, 1058–1065 (1961).
35. M.P. Gordin and G.M. Strelkov, "*About the extinction of CO_2-laser radiation by diffusively evaporating water droplet aerosol.*" Part 1. Preprint No. 22(171), Institute of Radio Electronics of the Academy of Sciences of the USSR, Moscow (1974).
36. M.P. Gordin, A.V. Sokolov, and G.M. Strelkov, "*About the extinction of CO_2-laser radiation by diffusely evaporating water droplet aerosol.*" Part 2, Preprint No. 28 (178), Institute of Radio Electronics of the Academy of Sciences of the USSR, Moscow (1974).
37. P.N. Svirkunov, Yu.S. Sedunov, and L.P. Semenov, Izv. Akad. Nauk SSSR, Fiz. Atmos. Okeana **16**, No. 5, 483–489 (1980).
38. R.Kh. Almaev, D.A. Volkovitskii, Yu.S. Sedunov, L.P. Semenov, and A.G. Slesarev, Infrared Phys. **25**, No. 1/2, 475–478 (1985).
39. E.L. Kogan, I.P. Mazin, ".N. Sergeev, and

V.I. Khvorost'yanov, *Numeral Modeling of Clouds* (Gidrometeoizdat, Moscow, 1984), 280 pp.
40. V.I. Khvorost'yanov, Meteorol. Gidrol., No. 3, 30–37 (1986).
41. R.Kh. Almaev, O.A. Volkovitskii, L.P. Semenov, and A.G. Slesarev, Meteorol. Gidrol., No. 4, 22–40 (1995).
42. I.P. Mazin and A.Kh. Khrgian, eds., *Clouds and Cloudy Atmosphere. Reference " ook* (Gidrometeoizdat, Leningrad, 1989), 647 pp.
43. R.G. Miake-Lye, M. Martinez-Sanchez, R.C. " rown, and C.E. Kolb, J. Aircraft **30**, No. 4, 467–469 (1993).
44. D.W. Fahey, E.R. Keim, et al., Science **270**, No. 5232, 70–74 (1995).
45. I.P. Mazin, Izv. Ross. Akad. Nauk, Fiz. Atmos. Okeana **32**, No. 1, 5–18 (1996).
46. A.N. Kucherov, "*Nonlinear interaction of a laser beam with the polydisperse water droplet aerosol*," Preprint No. 91, N.E. Zhukovskii Central Aerohydrodynamical Institute, Moscow (1996), 20 pp.

0235-6880/97/12 991-07